

Ocean Policy Studies

Contents

An analysis of Ocean Environment in the East China Sea
-A preliminary study on ocean environment assessment-

Fengjun Duan 1

On Flow Fields around an Outlying Island

Kazuyuki Maiwa 15

Joint Development of Mineral Resources on the Continental
Shelf

Akari Nakajima 119

各研究は、ボートレースの交付金による日本財団の助成金を受けて実施したものである。ここに関係各位に対し深謝申し上げます。

These projects were carried out under the patronage of The Nippon Foundation from the proceeds of motorboat racing. We would like to thank all those who made this possible.

Ocean Policy Studies

No.8 (November 2010)

Ocean Policy Research Foundation
Kaiyo Senpaku Bldg.,
1-15-16 Toranomon, Minato-ku, Tokyo 105-0001 Japan
Phone: +81-3-3502-1828
Facsimile: +81-3-3502-2033
E-mail: info@sof.or.jp
URL: <http://www.sof.or.jp>

Copyright

Ocean Policy Research Foundation

All rights reserved

No part of this publication may be used or reproduced in any manner whatever without written permission except in the case of brief quotations embodied in critical articles and reviews.

ISSN 1880-0017

EDITORIAL BOARD

Editor

Masahiro Akiyama Chairman, Ocean Policy Research Foundation

Editorial Advisory Board

Chua Thia-Eng Former Regional Director,
Partnerships in Environmental Management for the Seas of East Asia

Hiromitsu Kitagawa Former Professor, Hokkaido University

Tadao Kuribayashi Emeritus Professor, Keio University

Osamu Matsuda Emeritus Professor, Hiroshima University

Kunio Miyashita Emeritus Professor, Kobe University

Takeshi Nakazawa Professor, World Maritime University

Hajime Yamaguchi Professor, Tokyo University

An analysis of Ocean Environment in the East China Sea

-A preliminary study on ocean environment assessment-

Fengjun Duan*

Abstract

The temporal and spatial changes of the environment in the East China Sea (ECS), which is a semi-enclosed area bordered by China's Mainland and Ryukyu Islands and the largest continental marginal sea in the Western Pacific, are examined through the time series analyses of sea surface temperature (SST) and chlorophyll concentration data. The investigation results of the SST since July 2002 indicate a significant ocean surface warming. The spatial analyses suggest that it is driven by not only the large scale environmental change such as global warming, but also several local factors, for instance, the change of the discharge of the Yangtze River. In addition, the shallow ocean depth and the semi-enclosed water circumstance enlarge the magnitude of the surface warming. On the other hand, the analyses results of surface chlorophyll concentration since September 1997 detect a slight degradation in the ecosystem. Regional analyses indicate that the extent of the degradation is mainly depended on the changes of Yangtze River's discharges due to the filling process of the TGD reservoir.

Key words: the East China Sea, environmental change, sea surface temperature, chlorophyll, river discharge

1. Introduction

The East China Sea (ECS) is a semi-enclosed area bordered by China's Mainland and Ryukyu Islands. It connects with the Japan Sea by the Tsushima Strait in the Northeast, the South China Sea by the Taiwan Strait in the South, North Pacific Ocean through the Ryukyu Straits in the East, and adjacent to the Yellow Sea in the North (Fig. 1). Being the largest continental marginal sea in the Western Pacific, the ECS has a very complicated bathymetry. Its western part is occupied by the continental shelf covering about two thirds of the total area, and the

southern part is occupied by the continental slope and the deep Okinawa Trough (Fig. 1).

The marine environment of the ECS is governed by the ocean current system, air-sea interaction, and the river discharges. The Kuroshio runs into the ECS from the east of Taiwan Island, flows northeastward along the edge of the continental shelf, and then leaves through the Tokaro Strait southwest of Kyushu. With a relative stable route and volume, this strong current brings warm saline water into the ECS, and forms the eastern water boundary at the meanwhile. The Taiwan Warm Current runs into the ECS from the Taiwan Strait, flows

*Ocean Policy Research Foundation
2009.9.25 submitted; 2009.12.22 accepted

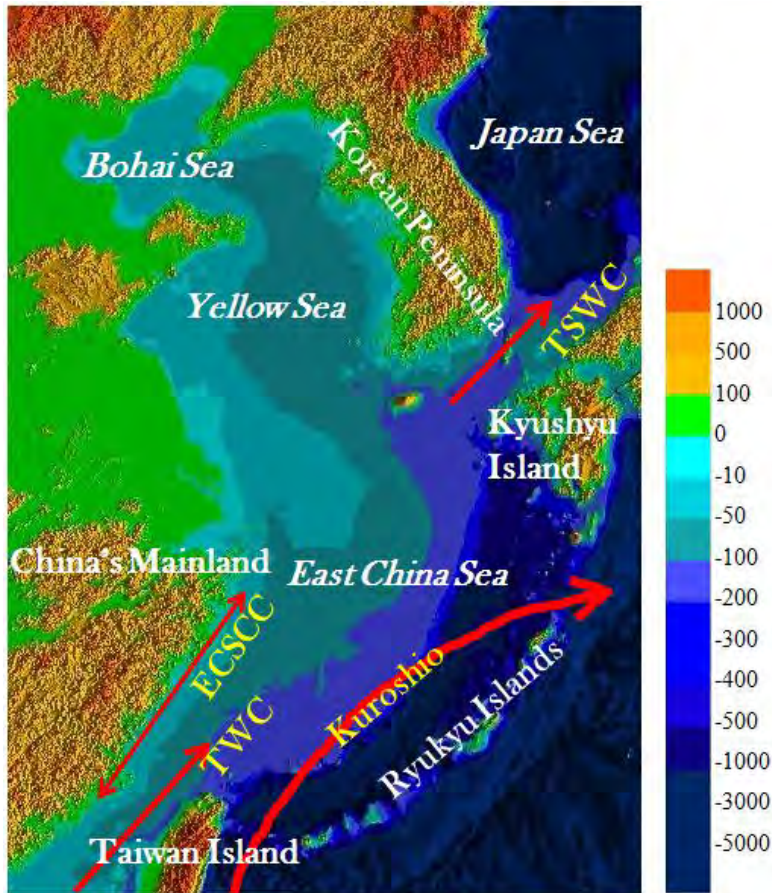


Figure 1 The location, topography and schematic ocean current system in East China Sea (shaded topography is created based on the GEBCO data, TWC, ECSCC and TSWC indicate the Taiwan Warm Current, the East China Sea Coastal Current, and the Tsushima Warm Current, respectively)

northeastward to the interior of the continental shelf. A coastal current along the western coast changes direction seasonally driven by the monsoon. The interior flow pattern is dominated by strong semidiurnal M2 (principal lunar semi-diurnal tide) tidal currents with superimposition of semidiurnal S2 (principal solar semi-diurnal tide), and diurnal O1 (principal lunar diurnal tide) and K1 (luni-solar diurnal tide) currents. The Tsushima Warm Current originates from the mixing between

water bodies of the ECS and the Yellow Sea, and flows to the Japan Sea through the Tsushima Strait. Atmosphere-sea interaction is responsible for vertical stratification of water masses in the ECS where the water is mixed vertically by strong surface cooling and wind mixing during winter and re-stratified by strong surface heating during summer. The water exchange between the coastal water and the Kuroshio Current tends to form a strong frontal zone between the warm and high salinity

Kuroshio Current and relatively cold and low salinity coastal ECS water at the shelf break. This front exhibits eddies due to baroclinic instability. The seasonal cycle of freshwater discharge, which mainly comes from Yangtze River along the east coast of China's Mainland, dominates the surface distribution of water thermal properties in the ECS, especially in summer when the river inflow is largest.

The Large Marine Ecosystem (LME) in the ECS is a productive one with shallow coastal waters that provide spawning and nursery grounds for many species of pelagic fish. The annual primary productivity is more than 300 gram carbon per square meter (NOAA, 2008), and is influenced by water temperature and by runoff from the major rivers coming from China's Mainland. The rivers deliver nutrients that affect the composition, distribution and dynamics of the phytoplankton population.

In the past several decades, the ECS environment has faced huge stresses from anthropogenic activities in the Yangtze River drainage basin and the coastal areas. Significant increase in nutrient loading caused high-frequently occurrence of red tide. Pollutants constitute a threat to coastal and marine ecosystem as well as to the health of coastal inhabitants. In addition, the Three Gorge Dam (TGD), the south to north water transfer project, and the global warming will impact the LME in the ECS. Some research have been carried out to examine these impacts individually (e.g., Chen, et al., 2003, D. Li and D. Daler, 2004, Jiao, et al., 2007, Chen, et al.,

2008). However, an integrated analysis for the ocean environment is necessary to protect marine ecosystem and to secure and support sustainable development, the economy, and the environment in the countries around the ECS.

2. Data and preprocessing

Three datasets were collected for this preliminary analysis on the ocean environment of the ECS.

The topography data comes from General Bathymetric Chart of the Oceans (GEBCO). It is a one minute global gridded dataset. The data for the study area (the ECS and surrounding areas (Fig. 1) was cut and loaded into a GIS system for the further analysis.

A Sea Surface Temperature (SST) dataset, so called New Generation Sea Surface Temperature, was used in this analysis. It is retrieved based on the satellite infrared observation (AVHRR¹, MODIS²) and microwave observation (AMSR-E³). Using the satellite-derived SSTs, a first guess (mean SST weighted by the auto-correlations in an observational window) is calculated, and then the grid SSTs are produced through an optimum interpolation scheme with de-correlation scales of 200km in latitude/longitude directions and 5 days in time. The compiled dataset is distributed through internet⁴. The dataset covers the area of 13-63N, 116-166E with a 0.05 degree grid. The temporal coverage is from July 2002 to real time with one day interval. The SST dataset was also cut and converted to GIS format for the further analysis.

In order to examine the ecosystem feature of the ECS, a dataset on primary productivity

1. Advanced Very High Resolution Radiometer

2. Moderate resolution Imaging Spectroradiometer

3. Advanced Microwave Scanning Radiometer - Earth Observing System

4. <http://www.ocean.caos.tohoku.ac.jp/~merge/sstbinary/actvalbm.cgi>

was include in this analysis. The dataset, named Level-3 global Standard Mapped Images, is compiled by Goddard Space Flight Center, National Aeronautics and Space Administration (NASA). The chlorophyll concentration is retrieved from observation by the SeaWiFS instrument onboard the SeaStar Spacecraft. Data is available from September 1997 till real time with spatial resolutions of 4-km and 9-km, and several time intervals. Limited by the swath width and the influence of clouds, the availability of the datasets with short time intervals are limited. Therefore, monthly average data with a 4-km grid size was selected to be used in this analysis. The area cut and format conversion were also carried out before the further analysis.

A GIS database including the three datasets was constructed together with several

base maps. Figure 2 shows the “areas of interest” (AOI) in this study. The range of the ECS was determined according to the definition of East China Sea Large Marine Ecosystem (NOAA, 2008). Four sub-areas were defined based on the topography and current pattern. Area 1 includes the estuary of the Yangtze River and surrounding area with the ocean depth less than 100 meters. Strong influence by the discharge of Yangtze River appears in this area. Area 2 occupies the continental shelf from southern to the central ECS. It is a water exchange area among the Changjiang Diluted Water (CDW), TWC, and the Kuroshio. Area 3 covers the Okinawa Trough, in which the Kuroshio flows. Area 4 is the upstream area of TSWC. Temporal and spatial analyses on the SST and primary productivity for these AOIs were performed.



Figure 2 The AOIs (area of interests) defined in this paper (refer to the text for detailed explanation)

3. Analysis results

3.1 SST changes in the ECS

The annual, seasonal and monthly mean SSTs of the entire ECS, sub-areas, and the 0.05 degree grids were calculated to examine the SST feature and changes. In general, there is a clear seasonal circle of the SST in the ECS (Fig. 3). During the winter (January to March), the average SST is about 17 to 19 degrees Celsius. After the warming up in spring (April to June), it rises to 27-30 °C during the summer (July to September). Then it falls again due to the cooling down in autumn (October to December). The seasonal difference of SST in the shallow western part of the ECS is greater than that of the deeper eastern part. It is a typical feature of continental marginal sea in sub-tropical area.

The route of the Kuroshio can be distinguished from the SST maps of January and April, but it is not so clear during the July and October because of the high SSTs in its surrounding area (Fig. 4). There is an SST gradient from southeast to northwest through all seasons. The contours in the northern part have relative stable direction almost paralleling to the route of the Kuroshio, which shows the influence to the adjacent area by the strong warm current. However, the contours show a clockwise rotation in spring to summer compared with the ones in autumn to winter in the southern part (Fig. 4). This phenomenon indicates the influence of coastal current driven by the monsoon. The northwestward summer monsoon generates a northward coastal current thereby the warmer water intrudes into the northern coastal area. During the winter monsoon season, a southward

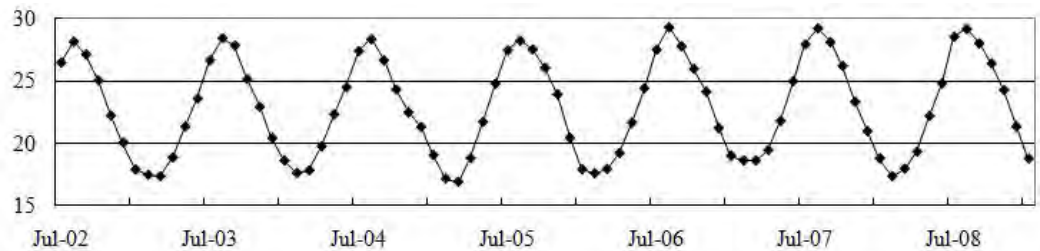


Figure 3 The monthly mean SST changes in the ECS (in degrees Celsius)

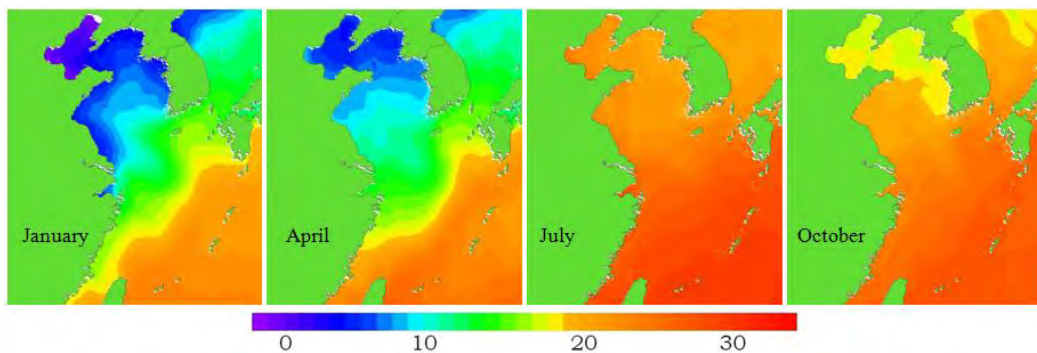


Figure 4 SST maps in 2003 (in degrees Celsius)

coastal current is generated, and the coastal area is occupied by the colder water.

Compared with the changes of surface temperature in the oceans of the Northern Hemisphere (Fig. 5(a)) and in the Northern Sub-tropical Area (Fig. 5(b)), annual mean SST change in the ECS (Fig. 5(c)) shows a continuous increase from 2003. The magnitude of the regional SST change exceeds to the six times of the ones in large scales. The reason

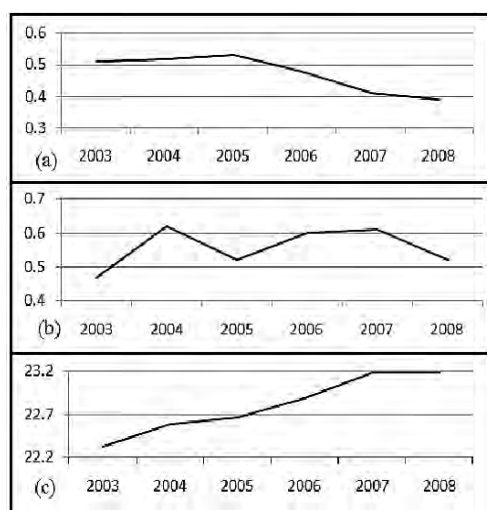


Figure 5 Comparison of the surface temperature changes among the Northern Hemisphere, Northern Sub-tropical Area, and the ECS ((a) shows the annual mean SST anomalies (in degrees Celsius, departures from the 20th century average) in the Northern Hemisphere (created based on the data from National Climatic Data Center, NOAA); (b) shows the annual mean Land-ocean Temperature Index anomalies (in degrees Celsius, departures from the average of 1951-1980) in Northern Sub-tropical area (24-44N) (created based on the data from GISS, NASA); and (c) shows the annual mean SST (in degrees Celsius) in the ECS)

for this difference can be explained by the low thermal capacity of the ECS due to the shallow ocean depth. Therefore the heating effect is enlarged, and the semi-enclosed environment helps the condition to be preserved.

In order to examine the details of this apparent surface warming, the seasonal and regional mean SSTs are plotted in Figure 6. All sub-areas contribute to the surface warming in the ECS, although the SST increase in the continental shelf (area 1 and 4) is a slightly larger than in deeper ocean (area 2 and 3). This similar surface warming in the whole ECS indicates the effect of global warming. Seasonally, it is clear that the strong warming occurs during summer and autumn. There is also a slight warming during winter, but no obvious SST increase during spring.

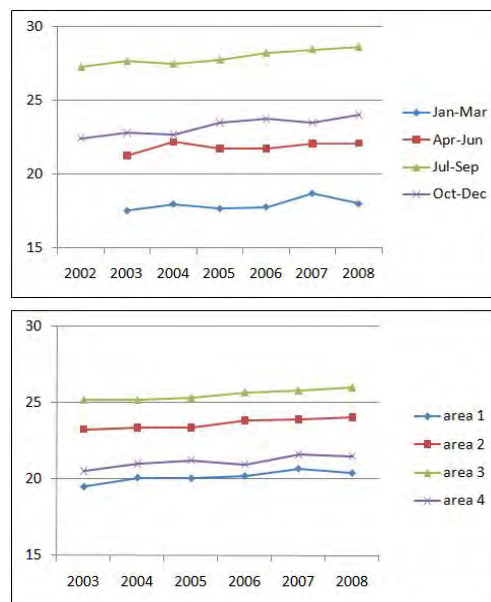


Figure 6 Seasonal (up) and regional (down) mean SSTs in the ECS (in degrees Celsius)

The seasonal difference of SST changes in the ECS was examined through the comparison of SST distributions between the earlier and later stages during the analysis period (Figs. 7 and 8). As mentioned above, the ECS water comes from several sources, those are the Kuroshio transport in the east, the TWC inflow from the Taiwan Strait in the south, the river discharge in the west, and the coastal current from the Yellow Sea during cold season in the north. Variability of these water sources also affects the SST in the ECS seasonally and locally. The main stream of the Kuroshio flows with a considerable stableness along the eastern boundary through all the seasons. Therefore there is no significant warming impact on the interior ECS by the strong warm current. A warming trend of itself occurs in warmer seasons, especially in

summer. However, the contribution to the regional surface warming is very low during colder seasons. On the other hand, the current system along the western coast shows quite different patterns. The SST distributions indicate a more strong northward coastal current during spring and summer. The warm water intrusion into the continental shelf contributes to the regional warming during the following season. A previous research (X. Tang, et al., 2009) reported significant warming trends in the ECS in both summer and winter during 1957-96 through the analyses of the hydrographic observation data. It is also noted that the warming in summer is primarily influenced by intensification of the TWC caused by the strengthening of the Kuroshio transport, while the warming in winter was mainly induced by the variability of the

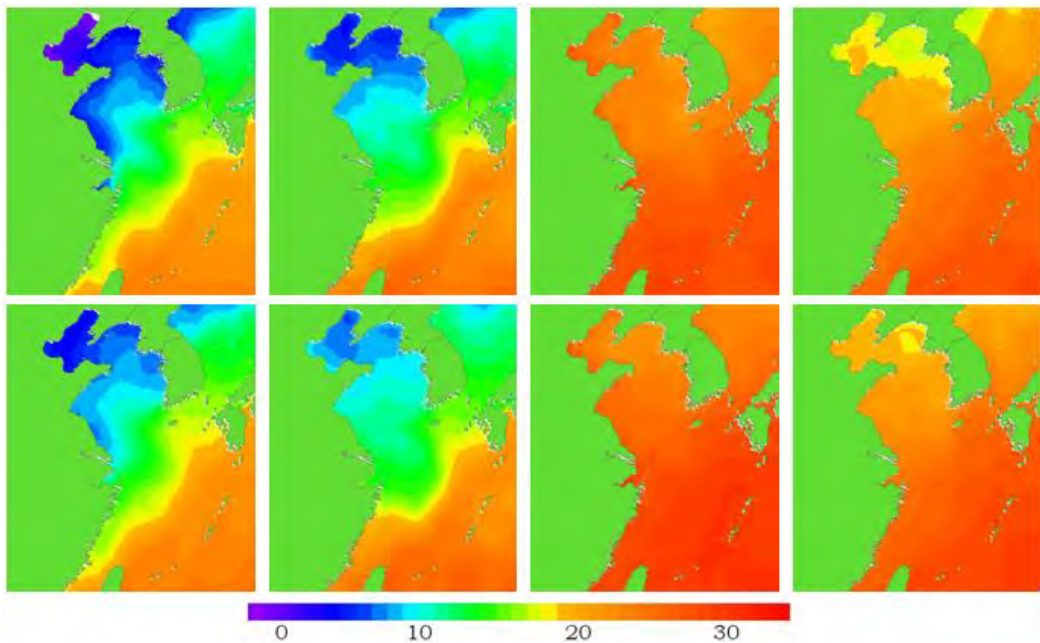


Figure 7 The SST distributions in the ECS and its surrounding area (in degrees Celsius)
 (Top (from left to right): January 2003, April 2003, July 2002, October 2002)
 (Bottom (from left to right): January, April, July, October 2008)

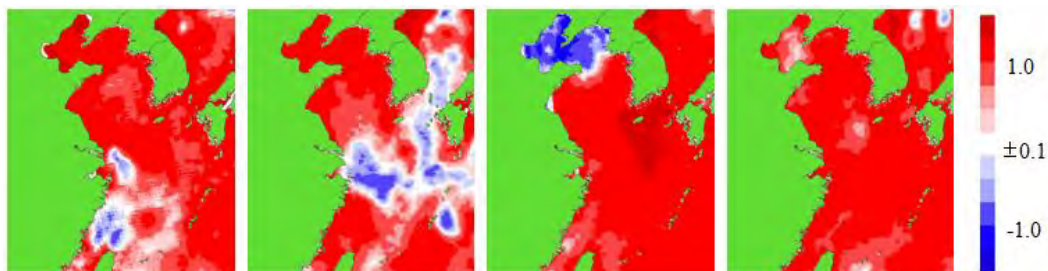


Figure 8 The SST differences in the ECS and its surrounding area (the differences between the two series shown in Figure 7, bottom-top)

climate system. Another influence factor that cannot be neglected is the change of river discharge. Low salinity water from the Yangtze River helps the stratification in the estuary and surrounding area, and there by the effects of summer surface heating and winter surface cooling are enlarged. In addition, the Yangtze River discharge strongly affects the ECS regional circulation during summer. As a result of the large-scale adjustment, the TWC and

coastal current are intensified, and the diluted water can be carried eastward over the continental shelf. The low salinity water lens will influence the SST of the central ECS in the following fall. The large annual variability of the river runoff influences the distribution of the lens. Consequently, during the seasons without strong surface heating, the SST in the central ECS fluctuates year by year (Fig. 9).

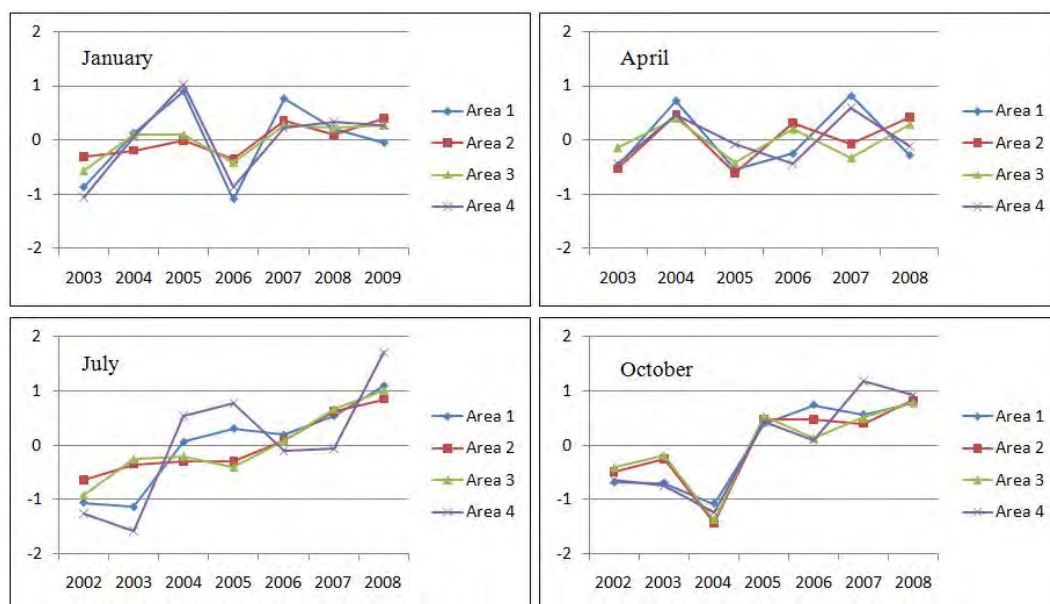


Figure 9 The Sub-regional mean SST anomalies in the ECS

3.2 Primary productivity changes in the ECS

The primary productivity in the ECS is governed by the temperature and the river discharges from the China's mainland. There are two blooms within a seasonal circle (Fig. 10). During winter, the strong vertical mixing generates a high density of nutrients in the top layer within the wide continental shelf. In April, with the increase of surface temperature, a spring bloom occurs due to these nutrients. The magnitude of the chlorophyll concentration is not

so large (1-10 mg/m^3), but the production happens over a wide area (Fig. 11). After the consumption of nutrients, the productivity decreases in the following several months. In July, the increased river discharges bring a large amount of nutrients into the ECS thereby a summer bloom occurs in the narrow coastal area, especially in the estuary of the Yangtze River (Fig. 11). The strong bloom can generate a very high chlorophyll concentration (over 30 mg/m^3), and form a red tide that can be harmful if their

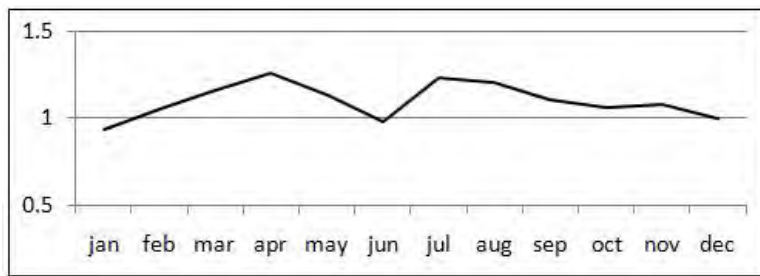


Figure 10 Average monthly mean chlorophyll concentration in the ECS from 1997 to 2008 (mg/m^3)

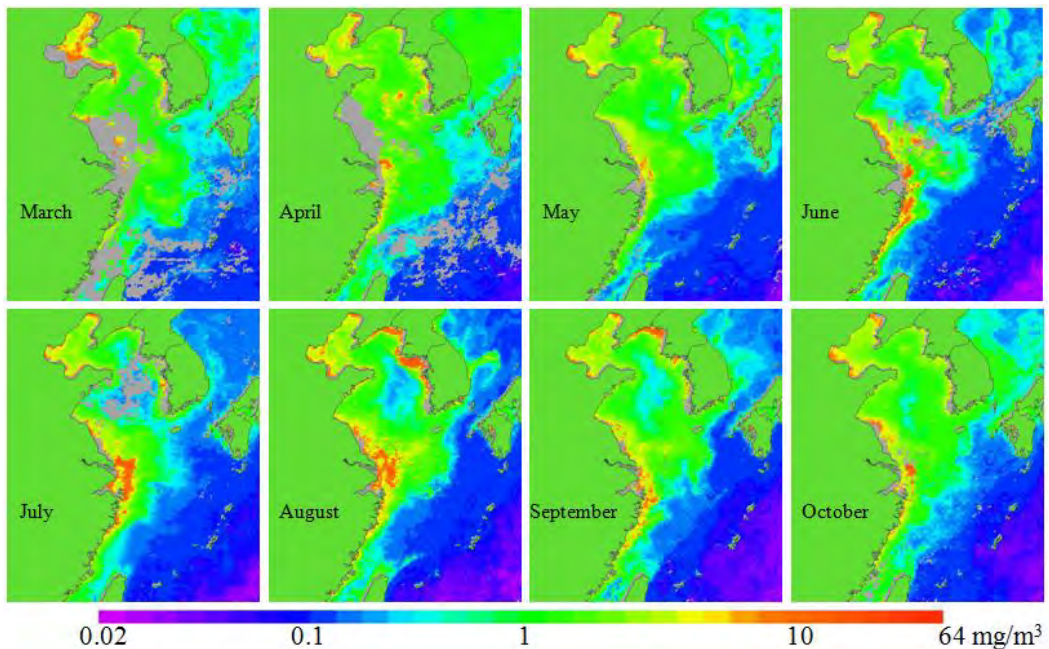


Figure 11 Monthly mean chlorophyll concentrations in the ECS from March to October of 2007

dissipation and senescence depletes the oxygen in the water, leading to massive mortality of fish and other important aquatic species.

Within the decadal analysis period, the annual primary productivity shows a slight decrease trend (Fig. 12). The magnitude might be 6-7% per decade. Regional analyses indicate that the ecosystem degradation occurs mainly in the continental shelf including the estuary of the Yangtze River (Fig. 12). Despite the relative large annual fluctuation, the productivity in Area 1 shows an obvious decrease (up to 15-20% per decade). Meanwhile, there was a bottom decrease observed between the first and second half of the decade with the margin of 2003 to 2004. The filling of the TGD reservoir started in June 2003 thereby the discharge from the Yangtze River, especially its seasonal distributions has been changed significantly. Within the filling period, the runoff of the

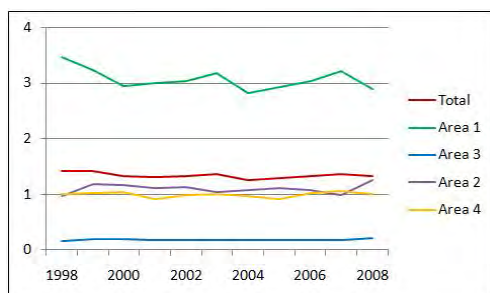


Figure 12 Annual mean chlorophyll concentrations in the ECS and the sub-areas (mg/m^3)

Yangtze River decreases especially in the dry season. The nutrients transported to the ECS will also decrease, and the surface nutrients density will decrease in the next spring. As a result, the spring bloom in April will be weakened. On the other hand, the discharge of the Yangtze River does not decrease significantly, and does not influence the summer bloom in coastal area (Fig. 13). Annual anomalies of surface chlorophyll concentrations reflect such bloom features very well (Fig. 14).

4. Discussion and concluding remarks

The environment and energy problem represented by global warming is one of the most serious problems that human beings will face to during the 21st century. Ocean will play an essential role to solve this kind of problem. It has the natural cleaning ability to absorb the pollution substances generated on the land, provides spaces to isolate carbon dioxide to relieve the global warming process, and can be beneficial to environment protection of land area indirectly. As to energy, not only the submarine oil, gas and methane hydrate, but also the offshore wind, ocean current and tidal current are coming to become very important energy supply. However, anthropogenic activities burden the ocean with the environmental load to the ocean area. Local environmental problems or even the large marine ecosystem problems might occur when the loads go beyond the biological

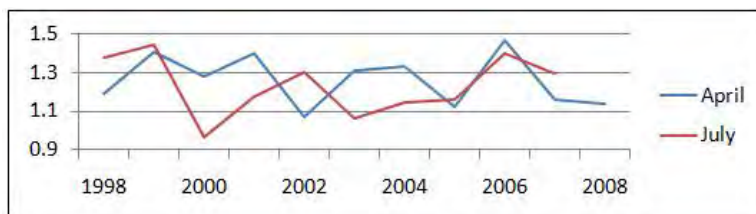


Fig 13 Seasonal mean chlorophyll concentrations in Area 1 (mg/m^3)

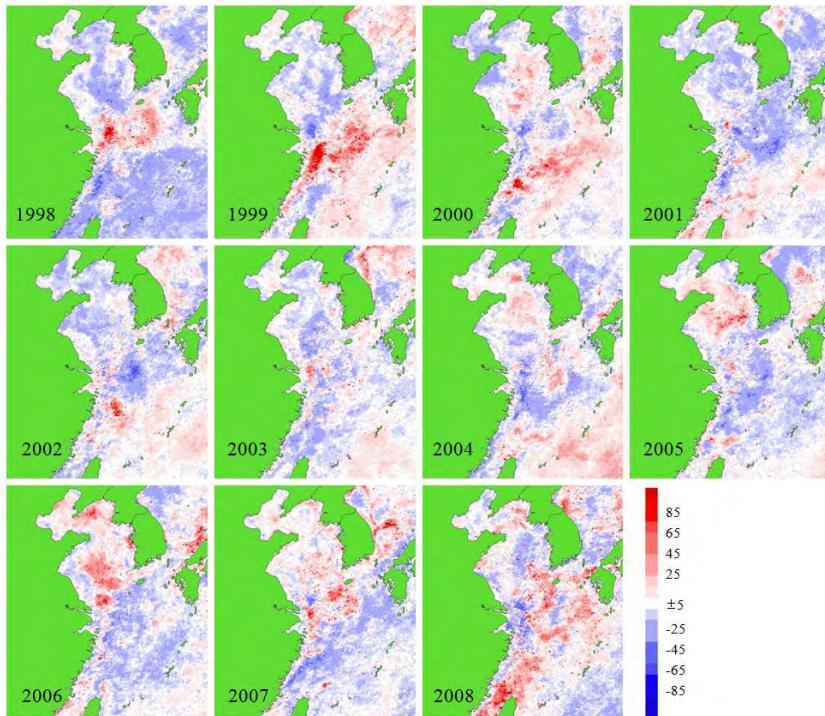


Figure 14 Annual anomalies of chlorophyll concentrations in the ECS (in percentages, departures from the average of 1997 to 2008)

capacities of ocean. It will take enormous cost and time to restore the destroyed ocean environment.

To address the problem, the UN Conference on Environment and Development held in Rio de Janeiro in 1992 developed a framework, Agenda 21. It indicated the role and status of coastal resources and ecosystems, and discussed the necessity of developing more sustainable methods to use marine resources. These ambitions became part of the World Millennium Goals and were reconfirmed by the World Summit on Sustainable Development (WSSD) in Johannesburg in 2002. The most essential principle of the framework is that the development and utilization of ocean area have to be carried out in harmonious with the environment to ensure the sustainability and the

possibility of enjoyment in the future. For the purpose, a clear picture, which could show the current status, potential and possible impacts by future actions, is crucial for establishing effectual policies to cope with both ocean development and environment protection. Recently, so-called best practices have been performed globally, regionally and locally (e.g. Millennium Ecosystem Assessment, Biological Assessment Report of the Yellow Sea, A Biogeographic Assessment off North/Central California). However, there has been few analyses in detail of the ECS due to poor observation data and some political reasons.

In this paper, time series SST and chlorophyll data were analyzed for examining the temporal and spatial changes of the ECS environment. A significant surface warming

being driven by not only the large scale environmental change such as global warming, but also several local factors such as the change of the discharge of the Yangtze River, was detected from the analyses. In addition, the shallow ocean depth and the semi-enclosed water condition enlarges the magnitude of the surface warming. On the other hand, ecosystem degradation during the last decade was observed to some extent through the analyses on surface chlorophyll concentrations. Regional analyses suggest that the degradation is mainly depended on the changes of Yangtze River's discharges caused by the filling process of the TGD reser-voir.

It is well discussed that the pollutants from land-based sources will damage the ecosystem in the ECS (e.g. Chen et al., 2003; D. Li and D. Daler, 2004). However, the large scale water utilization projects along the Yangtze River, such as the TGD and water transfer from Southern to Northern China, perhaps will impact the marine ecosystem the more seriously. These water utilization projects will not only reduce the total discharge, but also influence the seasonal discharge pattern, and thereby, impact the local ecosystem in the ECS which is stabilized by the present discharge volume and material flux in dry and flood seasons. An observation project (Jiao, et al., 2007) detected a sudden decrease of primary productivity in the ECS right after the first filling stage of the TGD in June 2003. The time series investigation is necessary to understand the synthetic impact of this big project on the ecosystem in the ECS. In addition, further comprehensive studies on the expected impacts should be carried out to work out sound countermeasures for sustainable

development of the region, including issues on the fisheries and the coastal fish-raising industry.

Acknowledgement

The topography data used in this paper was obtained from General Bathymetric Chart of the Oceans (GEBCO); the SST datasets were obtained from New Generation Sea Surface Temperature Development Group; and the SeaWiFS data were obtained from Goddard Space Flight Center, National Aeronautics and Space Administration. The author would like to thank the persons concerned.

References

- Xiaohui Tang, et al., Warming trend in northern East China Sea in recent four decades, *Chinese Journal of Oceanology and Limnology*, Vol. 27, Issue 2, pp.185-191, 2009
- Changsheng Chen, et al., Physical-biological sources for dense algal blooms near the Changjiang River, *Geophysical Research Letters*, Vol. 30, No. 10, 1515, doi: 10.1029/2002GL016391, 2003
- Daoji Li and Dag Daler, Ocean pollution from land-based sources: East China Sea, China, *Ambio* Vol. 33, No. 1-2, 2004
- Nianzhi Jiao, et al., Ecological anomalies in the East China Sea: impacts of the Three Gorges Dam? *Water Research*, 41, 1287-1293, 2007
- Changsheng Chen, et al. Physical mechanisms for the offshore detachment of the Changjiang Diluted Water in the East China Sea, *Journal of Geophysical Research*, Vol. 113, C2002, doi:10.1029, 2008
- NOAA, East China Sea large marine ecosystem, in *Encyclopedia of Earth*, eds. Cutler J. Cleveland, 2008

On Flow Fields around an Outlying Island

Kazuyuki Maiwa *

Abstract

The characteristics of physical fields around a table reef, as represented by Okinotorishima Island, are investigated using observed data and regionally idealised numerical models. Analysis of the data observed for Okinotorishima Island shows that tidal variation dominates sea level variation, and temperature difference between day and night at the point of observation is small compared with the case of the Shiraho reef.

A nesting scheme in numerical models is effective in resolving flow fields in reef areas, given the effects of the open ocean, though a finer resolution model requires the appropriate setting of a model domain. Numerical model results with realistic topography of Okinotorishima Island show that water flows out of the southwestern channel with the ebb tide and enters the reef area with the flood tide. Supported by the results from observed data, this indicates that the variation of flow field in Okinotorishima Island mainly depends on the tidal motion.

Key words: coral reefs, table reef, Princeton Ocean Model, nesting, environmental conservation of Islands

1. Introduction

Zooxanthellate corals (reef-building corals) play an important role in forming rich and unique ecosystems (coral reef ecosystems) in tropical and sub-tropical sea areas with relatively low levels of nutrients (Fig 1) and also act as natural seawalls. However, recently, the system has been severely damaged by extensive and severe bleaching as a result of anomalously high sea surface temperature (SST)¹, red-soil runoff from land areas, and outbreaks of *Acanthaster planci* (Kayanne et al., 1999, Nadaoka and Harii, 2004). According to Bryant et al. (1998), about 60 % of the world's coral reefs are at risk from anthropogenic effects and climate changes.

Small island countries formed by atoll islands are highly vulnerable to sea level rise and their ecosystems are also affected by social problems, e.g., artificial land alteration, population increase, and pollution and dumping problems. With regard to conservation of coral reefs, therefore, information based on solid scientific research is critical, on understanding, for example, dispersion of planulae larvae, the physio-chemical mechanisms of water flow over wide areas of reefs and responses of corals to stress from high SST. In particular, physical fields in coral reefs need to be understood in more detail, as physical conditions are one of the key factors in determining community distributions of corals and their production rates.

*Ocean Policy Research Foundation
2009.4.21 submitted; 2009.9.30 accepted

1. e.g. 1997 and 1998 events

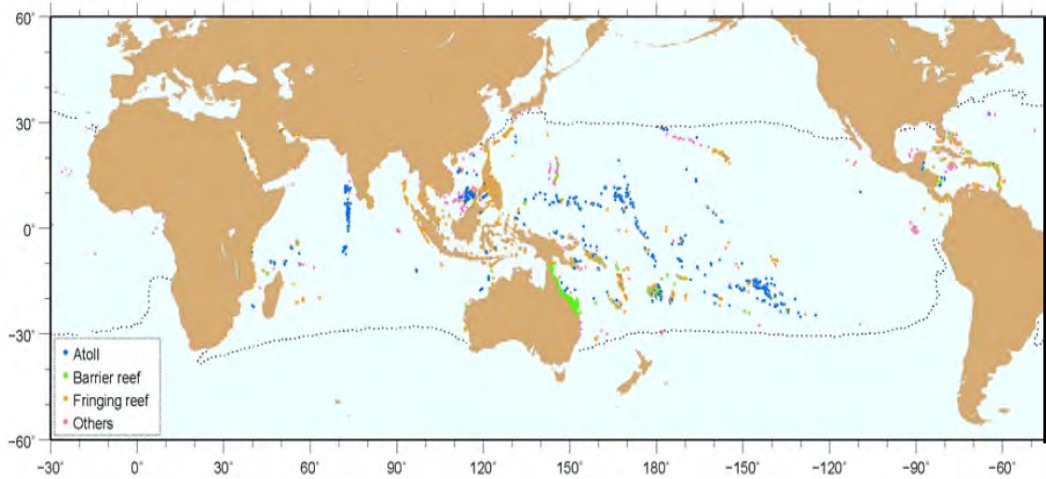


Figure 1: Distribution of world coral reef from Reef Base; the dotted lines show isotherm of 18°C of the annual mean SST

Coral reefs are basically classified into three types. First, fringing reefs grow in shallow waters and closely border on the coast. Most of the reefs in Japan belong to this type (e.g. Shiraho, Ishigaki Island). Secondly, barrier reefs are separated from land by lagoons of over about 10 m in depth. The Great Barrier Reef is the most well-known example of barrier reefs. Finally, atolls are circular or sub-circular in shape without a central land area, as seen in the Majuro atoll, within the territorial waters of the Republic of the Marshall Islands.

Coral reefs in Japan are mainly located around the Ryukyu Islands. Many past studies about coral reefs in Japan are on those in the region and have focused on the characteristics of flow and temperature (Suzuki et al., 2004, Tamura et al., 2004) and recovery of coral populations after bleaching events (Kayanne et al., 2002) there. For example, in a study on barrier reefs, Tamura et al. (2005) investigated the characteristics of heat and matter transport for the purpose of selecting Marine Protected Areas (MPAs) in Sekisei Shouko, Yaeyama Islands and

Mitsui et al. (2004) analysed observed data on the characteristics of the transport of planurae larvae in the same area. In a study on fringing reefs, Kumagaya et al. (2004) analysed observed data on the characteristics of current and temperature fields in Shiraho, Ishigaki Island. They demonstrated that temperature variations can be characterized by the four patterns, which are in accordance with the susceptibility of corals to high temperature. Tamura et al (2004) investigated the characteristics of current fields in the same field by use of the observed data and a numerical simulation. They showed that geomorphological effects are important for flow mechanisms in Shiraho reef.

There exist other types of coral reef in Japan, such as table reefs, represented by Okinotorishima Island or Yabiji Reef in Miyako Island. However, few studies have focused on this type of reef.

The objective of this study is to investigate the characteristics of physical fields around a table reef, as represented by Okinotorishima Island, using observed data and regionally

idealised numerical models.

The paper is composed of seven sections. After Section 1 of the introduction, in section 2, the data used in this study is briefly described and a description of a numerical model is given. Section 3 shows the results from some observed, elementary analyses. A simple numerical model is used in Section 4 as a possible suggestion for developing a suitable model for table reefs. Section 5 contains a discussion of tidal effects on the flow field in a table reef similar to Okinotorishima Island. A numerical model with more realistic bottom topography is used in this section. A summary and discussion of the study are presented in Section 6.

2. Data and Model Description

2.1 Data

The Japan Agency for Marine-Earth Science and Technology (JAMSTEC) has carried out the meteorological and oceanographic observations at Okinotorishima

Island since 1993. The meteorological data available are wind speed and direction, air temperature, humidity, air pressure, and solar and infrared radiations. The oceanographic data are water temperature, tide level by water pressure, and chlorophyll. The observation periods and intervals are listed in Table 1². The XBT/XCTD observations were also carried out³ during cruises for maintenance of observation devices from 1995 to 2000.

In Section 3, the characteristics of temperature and tidal variations in the moat are investigated using temperature and pressure data observed at a depth of 4 m. The data for 6 months, from 1 March to 31 August, 2002, have been selected, as they are the latest 6 month consecutive water pressure data available and are needed for harmonic analysis with 16 main tidal constituents. In section 4, the XCTD data are compared with the data from the high resolution OGCM⁴. In section 5, the data of wind speed and direction are used for wind forcing on the sea surface of the model.

Table 1: Observed data list in Okinotorishima Island

	item	period	Interval
Meteorology	Averaged and maximum wind velocities, wind direction, air temperature, humidity, air pressure, solar and infrared radiations	1993.4-1994.2	1 hour
		1994.2-2003.2	30 minutes
	Averaged and maximum wind velocities, wind direction, air temperature	2003.1-	30 minutes
Oceanography	Water temperature, water pressure, chlorophyll <i>a</i>	1996.2-2002.2	1 hour
	Water temperature, water pressure	2002.2-2003.1	1hour
	Water temperature	2003.1-	20 minutes

2. The data are obtained from <http://www.jamstec.go.jp/j/database/okitori/index.html>

3. The observations were also carried out by JAMSTEC.

4. JCOPE2 data, see Section 4.

2.2 Model description

The Princeton Ocean Model (POM) used in section 4 is a three-dimensional nonlinear primitive equation model with hydrostatic assumption (Blumberg and Mellor, 1987). The model incorporates a free surface explicitly and a terrain-following σ -coordinate in the vertical direction. The σ -coordinate is well considered to be appropriate to deal with interactions between bottom topography and ocean dynamics, especially in coastal regions with shallow continental shelves and continental slopes. Vertical diffusivities and viscosities are derived from the Mellor-Yamada turbulent closure submodel (Mellor and Yamada, 1982), while horizontal diffusivities and viscosities are parameterized based on the strain and stress tensor in the flow proposed by Smagorinsky (1963). To secure computational efficiency, a mode-splitting technique is adopted in the model, in which the vertically integrated equations (external mode) are calculated separately from the vertical structure equations (internal mode) (Blumberg and Mellor, 1987).

In order to take account of the effects of the open ocean around Okinotorishima Island in the model, a nesting technique is used in numerical calculations (Spall and Holland, 1991, Miyazawa and Minato, 2000). The nesting method can reduce computer resource usage by embedding finer resolution grids within a coarser grid, and performs well with 3:1 and 5:1 grid ratios (Michael and Holland, 1991). For the sake of simplicity, the one-way nesting is used in this study.

In Section 5, POM version 2008 is utilised. This latest version model can solve the wetting and drying (WAD) processes that might prevail in near-coast regions and is particularly suited for simulation of coral reef areas (Oey, 2005, 2006, Oey et al., 2007).

3. Tidal and Temperature Variations in Okinotorishima Island

3.1 Tidal variation

Sea level is obtained by the equation of the water pressure derived from the hydrostatic equation in which when a fluid is at rest and in equilibrium, and the pressure and the density of water are constant on the surface of constant height z , the body force is assumed to be balanced by the pressure force,

$$p = p_a + \rho g(\eta - z), \quad (1)$$

where z is depth, p_a the air pressure, ρ the density of water, g the acceleration due to gravity and η the sea level. Given the depth of the observed point, ($z = 4$ m) and air pressure from observed data and density ($= 1,025 \text{ kg/m}^3$), we obtain the sea level.

In order to obtain the tidal anomaly, the harmonic analysis was performed using the sea level derived from equation (1) and the main 16 tidal constituents for the period of six months from 1 March to 31 August, 2002. Table 2 shows the periods and frequencies for each constituent. The difference between the obtained sea level and the six-month mean gives the anomaly.

Figure 2 shows the time series of hourly sea level anomalies recorded at Okinotorishima Island during the period from 1 March to 31 August, 2002. The time series of the sea level clearly shows diurnal and semidiurnal variations throughout the period. The sea level has anomalously high peaks in early July, when typhoons (Typhoon CHATAAN, around 8 July; Typhoon HALONG, around 13 July, etc.) passed through the region of Okinotorishima Island around the period under observation. The solid line in Fig. 3 shows a part of the time series of the

Table 2: Main tidal constituents in the diurnal and semidiurnal tidal bands

Tidal constituent	Period	Frequency (cph)
Q_1	26h52m6.084s	0.0372
O_1	25h49m9.63s	0.0387
M_1	24h49m59.694s	0.0403
P_1	24h3m57.205s	0.0416
K_1	23h56m4.091s	0.0418
J_1	23h5m54.516s	0.0433
OO_1	22h18m21.867s	0.0448
$2N_2$	12h54m19.348s	0.0775
μ_2	12h52m18.327s	0.0777
N_2	12h39m30.054s	0.0790
ν_2	12h37m33.616s	0.0792
M_2	12h25m14.164s	0.0805
L_2	12h11m29.833s	0.082
T_2	12h0m59.217s	0.0832
S_2	12h0m0s	0.0833
K_2	11h58m2.045s	0.0836

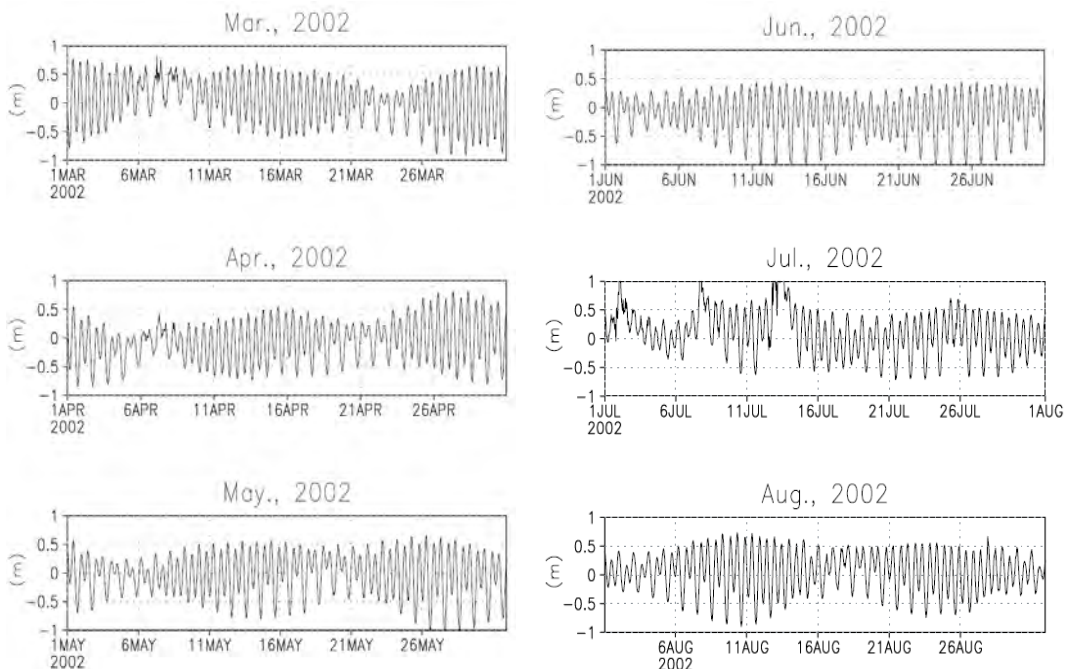


Figure 2: Hourly sea level anomaly recorded in Okinotorishima island. The series of the anomaly are calculated by the difference between the original 4416-h series and average of this period.

fitted tide anomalies obtained from a least-squares fit of 16 main tidal frequencies through the period from 05:00, 29 March to 04:00, 31 March, 2002. For comparison, a time series of sea level anomalies in the period is superimposed by a dashed (marked by +) line. As seen from this observed results in Fig. 3, sea level variation is dominated by the diurnal and semidiurnal tidal variations. The maximum amplitude of the tide anomaly through the total series is about 0.8 m. The standard deviation for the original record is 0.381 m while that for the fitted record is 0.342 m. For the period of the data record, the sum of the 16 tidal constituents accounts for about 90 % of the total variance in the record. The results here are used for a boundary condition in the experiment in Section 5.

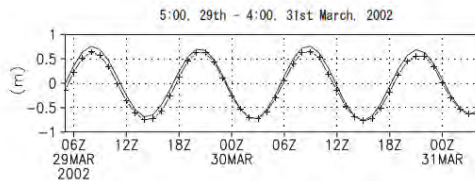


Figure 3: The solid line is the time series of fitted tide anomaly from 5:00, 29 to 4:00, 31 March, 2002, obtained from a least-squares fit of the 7 main diurnal and 9 main semidiurnal tidal frequencies. The dashed line (marked by +) is anomaly calculated by the original series.

3.2 Temperature variation

Figure 4 shows temperature time series observed at the depth of 4m in the moat at Okinotorishima Island. The temperature is at its maximum of $32^{\circ}C$ on 26 June. Temperature difference between day and night is about $1.7^{\circ}C$ at the observation point. Tamura et al. (2004) show that the difference in the moat of Shiraho reef is about $5^{\circ}C$, while the differences

in the other part of the reef are higher than in the moat. The difference in the moat at Okinotorishima Island is smaller than in Shiraho reef.

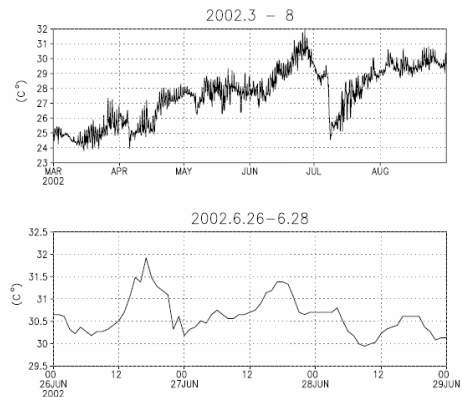


Figure 4: Hourly temperature time series recorded in Okinotorishima island (a) from 1 March to 31 August, 2002 and (b) from 26 to 28 June, 2002.

These data at Okinotorishima Island, however, are observed only at one point. Therefore, in order to understand the characteristics of spatial distribution and the variation of various time scales in detail, long-term observations at points with special topographical characteristics (e.g., reef crest and channel) are necessary. In addition to consideration of the dynamic effects on the reef, problems above will be improved at the next stage.

4. Numerical Experiments with Ideal Topography

In order to investigate the flow field around Okinotorishima Island, an Ocean General Circulation Model (OGCM), known as the Princeton Ocean Model (POM), is utilised. One-way nesting with a 3:1 grid ratio is applied to this model to take account of the effect of the open ocean on the reef scale.

4.1 Results with xy -independent basic profile of the initial conditions

Model domain is f -plane ($f = 4.54 \times 10^{-5} / s$) and $199.8 \text{ km} \times 199.8 \text{ km}$ (horizontal direction). The horizontal grid resolution of the coarse model is 2.7 km . The vertical grid varies over the domain with 15 levels covering the water column. An ideal seamount is specified as below,

$$H = 4500 - ((4000 / \exp(-1/ra^2)) \times \exp(-(((x - x_c) / L_x)^2 + ((y - y_c) / L_y)^2) / ra^2)) \quad (2)$$

where x is the longitude, y the latitude, (x_c, y_c) the centre of the domain, $ra = 20/3$, $L_x = 2.25 \text{ km}$ and $L_y = 1.0 \text{ km}$ (Fig.5). The maximum depth for the model is set at 4500 m . H is taken as 5 m when $H < 0$. All the data are stored daily and used in the following analyses. Each of the initial temperature and salinity fields has xy -independent basic profile and is expressed by:

$$T = 5.0 + 15 \times \exp(-z/1000) \text{ (}^\circ\text{C)}, \quad (3)$$

$$S = 35.0 \text{ (psu)}, \quad (4)$$

respectively, where z is the depth.

Figures 6 and 7 show sequential sea surface temperature and velocity field of coarse ($dx = dy = 2.7 \text{ km}$) and fine ($dx = dy = 0.9 \text{ km}$) grids around the island from Day 5 to Day 8, respectively. The results of the fine grid model show the finer structure, which cannot be resolved by the coarse grid model. For example, warm (cold) water in the eastern (western) part of the island is clearly seen. Figure 8 shows snapshots of the sea surface

temperature and velocity fields of the 900 m and 300 m grids at Day 8. The model with resolution of 300 m performed well. The results of the temperature show the separation of eddies around the island, which cannot be resolved by the 900 m resolution model.

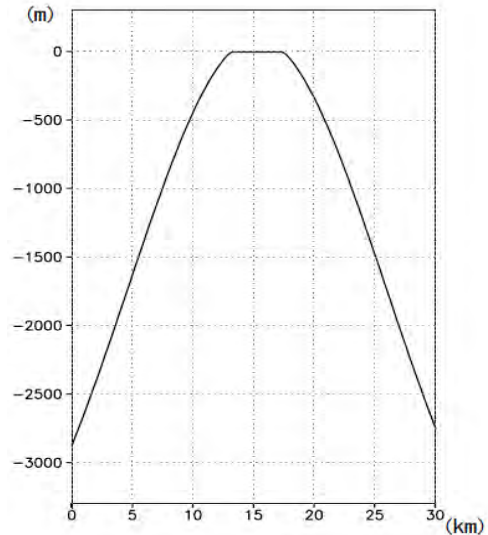


Figure 5: Seamount configuration

However, the model with 100 m resolution could not run because of the accumulation of water mass in the centre of the model domain where a wide area is occupied by relatively shallow depth compared with the one near the boundary, and resulting in an unrealistically large velocity.

Although realistic data for the vertical profile for the variables given to initial and boundary conditions around Okinotorishima Island are needed to avoid this problem, the data have not been observed. The results from the high resolution model are then used for both initial and boundary conditions in the next step.

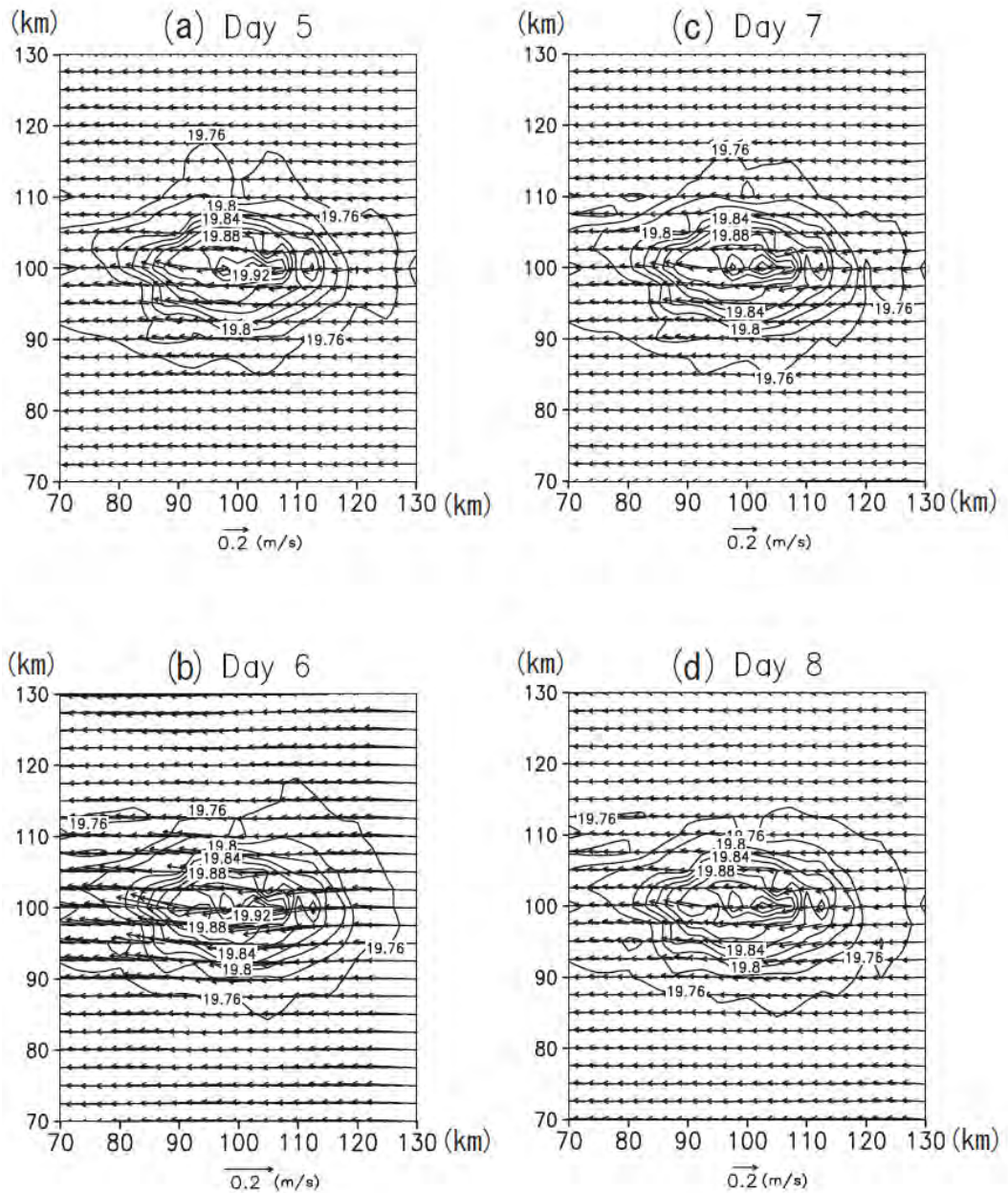


Figure 6: Sequence of the results from the numerical experiments with initial and boundary conditions of xy -independent basic profile. Sea surface temperature and velocity fields are shown in contours and velocity for the coarse grid (left; $dx=dy=2.7$ km) and the fine grid (right; $dx=dy=900$ m) at Day 8 in the model.

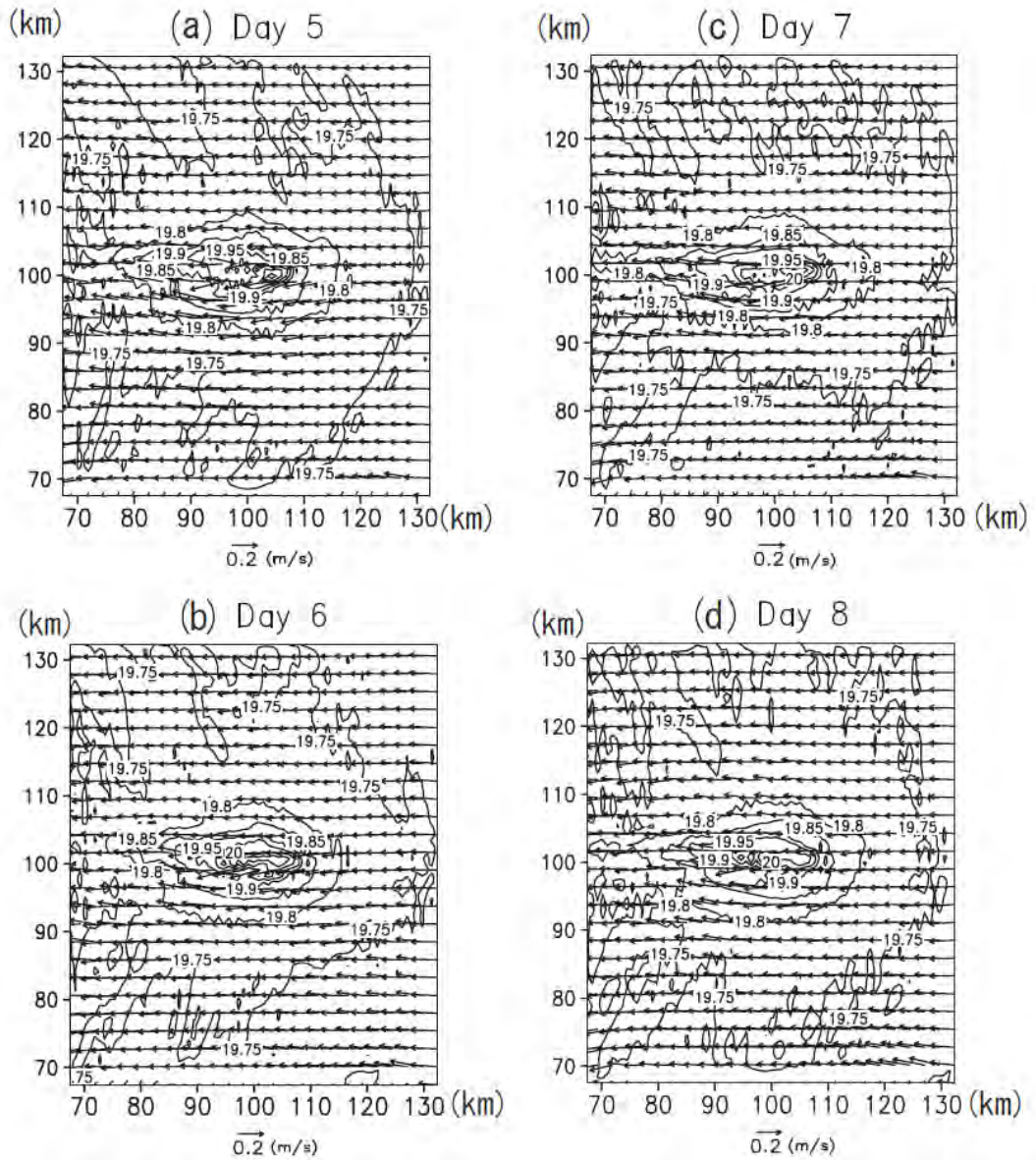


Figure 7: Same as Figure 6 but for fine resolution model ($dx=dy=900 \text{ m}$).

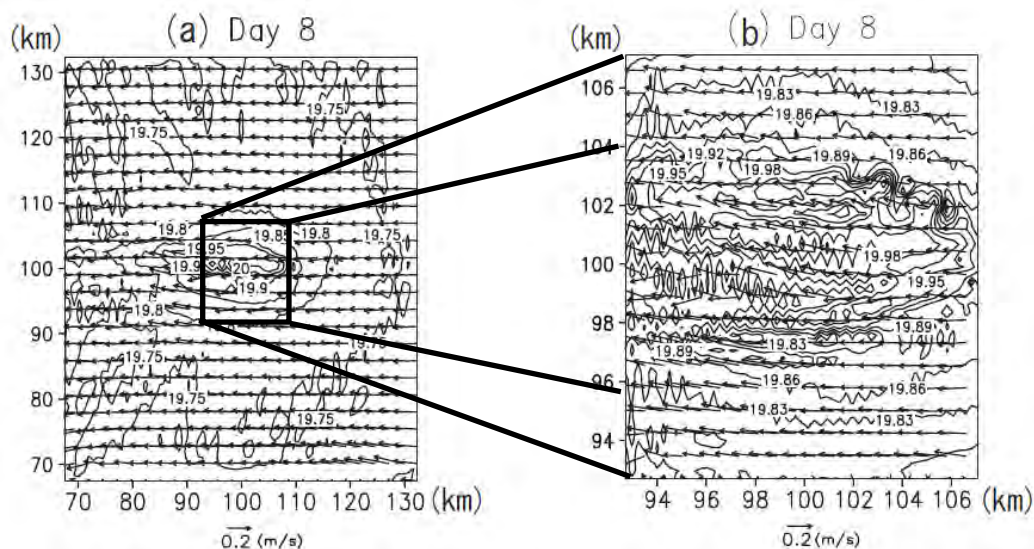


Figure 8: Comparison of sea surface temperature and velocity fields between the coarse grid (left; $dx=dy=900$ km) and the fine grid (right; $dx=dy=300$ m) at Day 8 in the model.

4.2 JCOPE2 Reanalysis

JCOPE system is a near operational forecasting system of the variability of the Kuroshio-Kuroshio extension path and has been developed by JAMSTEC since 1997. In collaboration with the Fishery Research Agency (FRA), this system has been developed to analyse the Kuroshio path variation south of Japan (JCOPE1; Miyazawa et al., 2008a; Kagimoto et al., 2008) and operated for management of fishery resources off Japan through development of coupling with ecosystem models since April, 2007 (FRA-JCOPE; Miyazawa et al., 2008b). Currently the system has been further developed by including enhanced model and data assimilation schemes (JCOPE2). The reanalysis dataset is produced by improving model results by use of various observed data from satellites, ARGO floats, and ships (data assimilation). The outputs of JCOPE2 capture the various ocean states around Japan. The reproduction of the ocean states in the Mixed

Water Region off North-East Japan has made great progress in its accuracy by the considerable efforts of the JCOPE Group community. The outputs are utilised for optimum routings of oil tankers, fishing boats, and decisions of work positions of drilling ships. Table 3 compares the detail of JCOPE2 with that of JCOPE1.

Figure 9 shows the Kuroshio and Kuroshio extension paths obtained from observed data (upper panels, Ambe et al., 2009) and the reanalysis data (lower panels). The result based on the reanalysis data well reproduces the activity of the Kuroshio path and the meander of the Kuroshio extension for each year. Figure 10 shows vertical sections of temperature obtained from XCTD observation in the cruise (left) and the reanalysis data (right) in February, 1998. Okinotorishima Island ($136^{\circ} 05' E$, $20^{\circ} 25' N$) is located near the left edge of the panels in Fig. 10. The vertical structure of the temperature is also well reproduced by the reanalysis data. The vertical structures not only

of temperature but also of salinity from the observed data are in good agreement with those

from the reanalysis data, although no figure is presented for salinity.

Table 3: Comparison between JCOPE1 and JCOPE2

	JCOPE1	JCOPE2
Source code	POMgcs (Mellor et al., 2002)	POMgcs
Horizontal resolution	1/12 degree	1/12 degree
Horizontal range	12-62N, 117-180E	10.5-62N, 108-180E
Vertical levels	45 levels (10m, 21m,.....)	47 levels (2m, 3m, 5m,)
Baroclinic pressure gradient scheme	Second order scheme (Mellor and Blunberg, 1987)	Fourth order scheme (McCalpin, 1994)
Tracer advection/diffusion schemes	Center difference Harmonic diffusion	Flux Corrected Transport Bi-harmonic diffusion
Nesting	Fixed to the boundary values	Flow Relaxation scheme
Surface heat flux	Coarse-reso, 'Reynolds' SST	High-reso, model SST
Topography	DTM5 (ETOPO5)	DTM5, JTOPO30 Uehara(2002), GEBCO
M2 tidal mixing	No	Lee and Matsuno (2007)
Changjiang discharge	No	Monthly observation

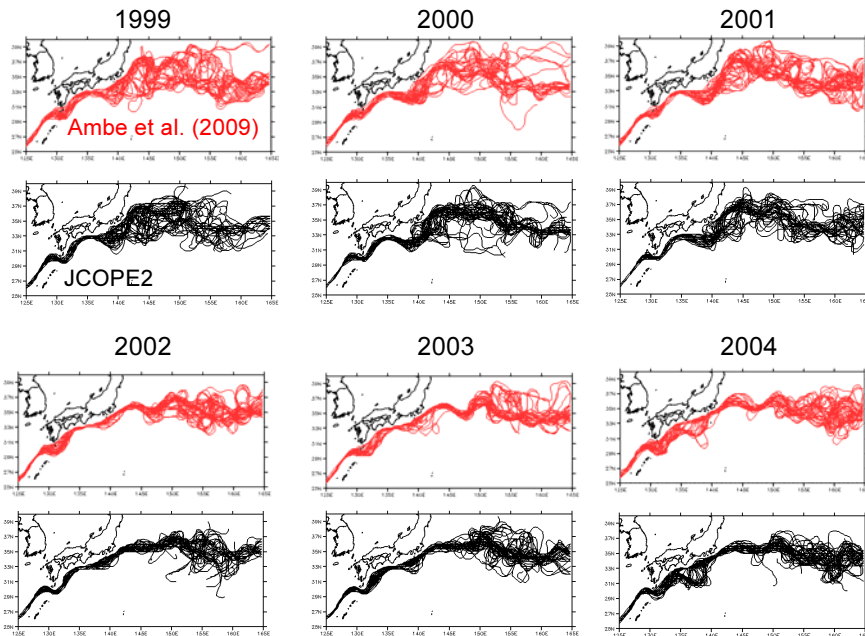
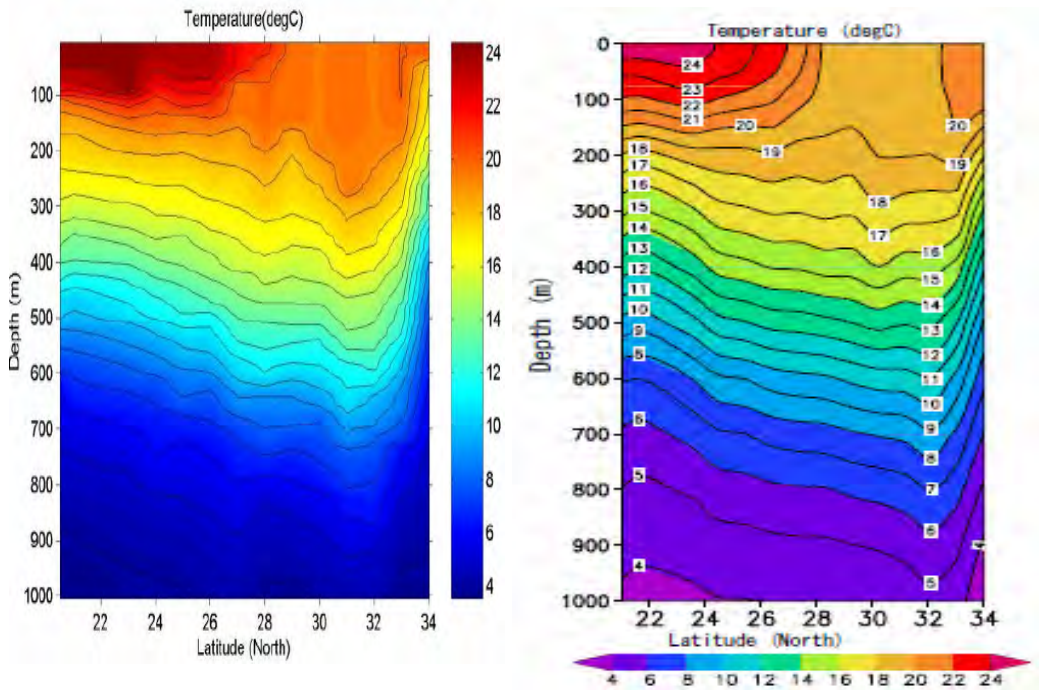


Figure 9: Comparison of Kuroshio-Kuroshio extension path between the results from observed data (upper panels) and the JCOPE2 reanalysis (lower panels) from 1999 to 2004.



(horizontal resolution; 2.7km × 2.7km).

Figure 10: The vertical sections of temperature obtained from observed data by XCTD in the cruise for maintenance of observation devices in Okinotorishima island (left panel) and the JCOPE2 reanalysis (right panel).

4.3 Results with the initial and boundary conditions using the reanalysis data

The results in the previous subsection showed the excellent reproduction of the reanalysis data to realistic ocean states. Therefore, the reanalysis data are used for the initial and boundary conditions in the numerical model in this subsection.

The model domain is the same as in the previous experiment except for horizontally 62.1 km × 62.1 km. Temperature, salinity and zonal and meridional components of velocity are horizontally averaged for each vertical level of the reanalysis data. These vertical profiles are used for the boundary and initial conditions in the coarse grid model

Figure 11 shows sea surface temperature and velocity fields for the coarse grid ($dx=dy=2.7$ km) and the fine grid ($dx=dy=900$ m) at Day 8. The fine structure is demonstrated plainly in the result of the grid as fine as 900 m sq. However, when the grid becomes finer than 900 m sq. up to 300 m, the computation fails to provide reasonable results.

Possible reasons for the computational error are:

- 1) coarse vertical resolution, that is, the pressure gradient error is sensitive to the vertical resolution (Haney, 1991); the error related to this can be improved by increasing the vertical levels, and
- 2) accumulation of water in the centre of the

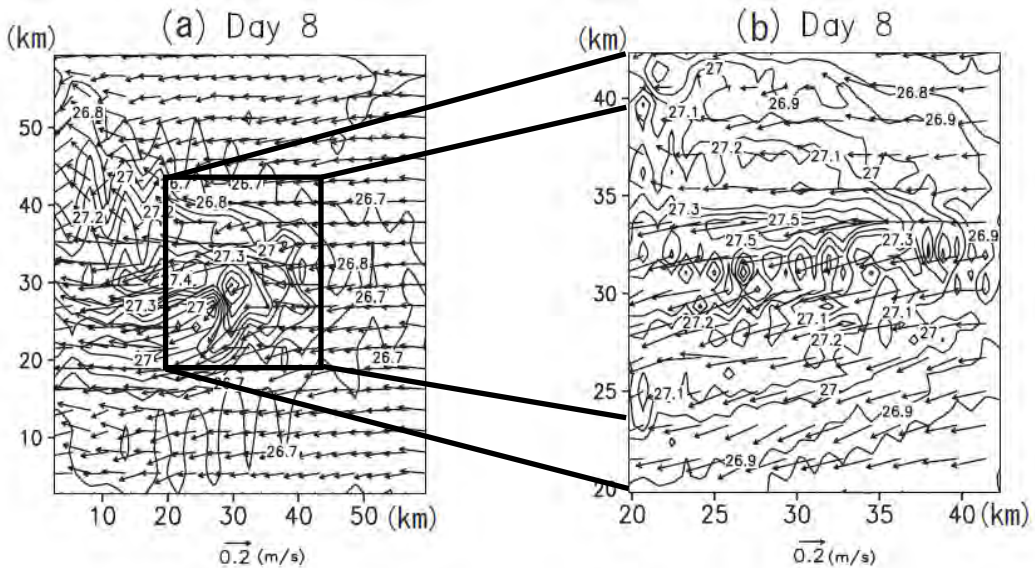


Figure 11: Results from the numerical experiments with a initial and boundary conditions from JCOPE2 reanalysis. Sea surface temperature and velocity fields are shown in contours and velocity for the coarse grid (left; $dx=dy=2.7$ km) and the fine grid (right; $dx=dy=900$ m) at Day 8 in the model.

numerical model domain where the depth is relatively shallow compared with the depth near the boundary, that is, abnormal velocity is computed around the centre of the domain; this problem can be improved by expanding the model domain of the fine grid model.

In order to obtain reasonable results in the simulation, the model domain should be appropriately set in consideration to the relation between topography, grid size and resolution.

5. A numerical experiment with realistic, local bottom topography

This chapter discusses the additional experiment performed. The model in this experiment is the latest version of POM that

can estimate submerged and exposed processes of topography (Oey, 2005, 2006, Oey et al., 2007) and is suitable for analyzing tidal effect.

The horizontal grid size is 66 m sq. The vertical resolution varies over the domain with 15 levels covering the water column. The bottom topography is reproduced from a chart of Okinotorishima Island (Fig. 12). For simplicity, the maximum depth is set to 50 m. The reanalysis data are used for the initial and boundary condition as in section 4.3. The main 16 tidal constituents obtained from the observed data in section 3.1 are taken into as an additional condition along the western boundary (Fig. 3). Sea surface is forced by the momentum flux observed from the observed wind data at Okinotorishima Island. In order to reduce the initial disturbance, the wind amplitude is supposed to be linearly increased during the first 24 hours.

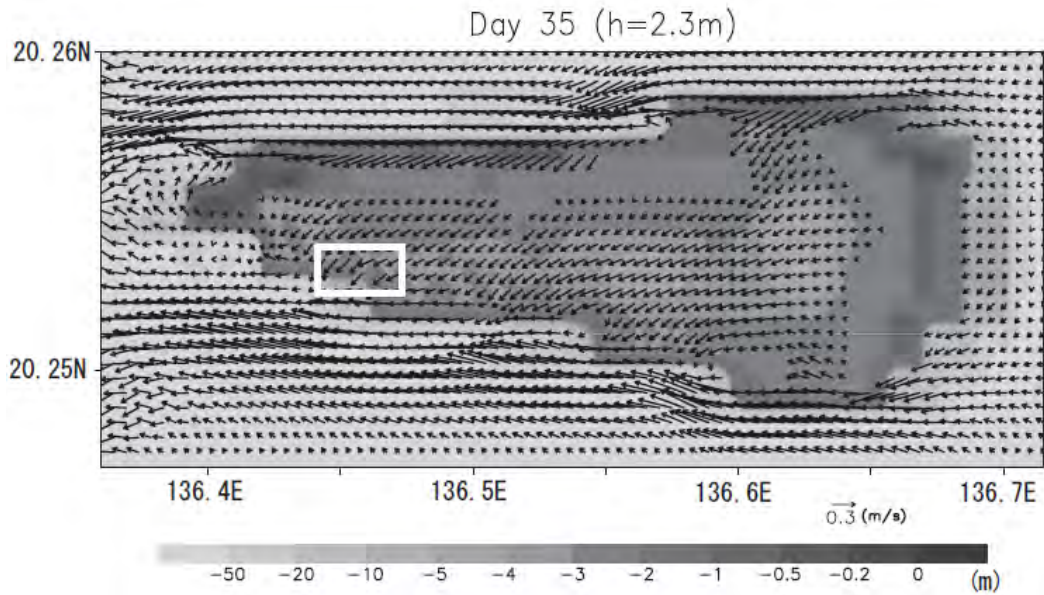


Figure 12: Result from numerical experiment with more idealistic topography and the 16 main tidal components. Velocity field is shown in arrows at 35-hour (on the ebb tide) at 2.3 m depth in the model with the bottom topography in shade.

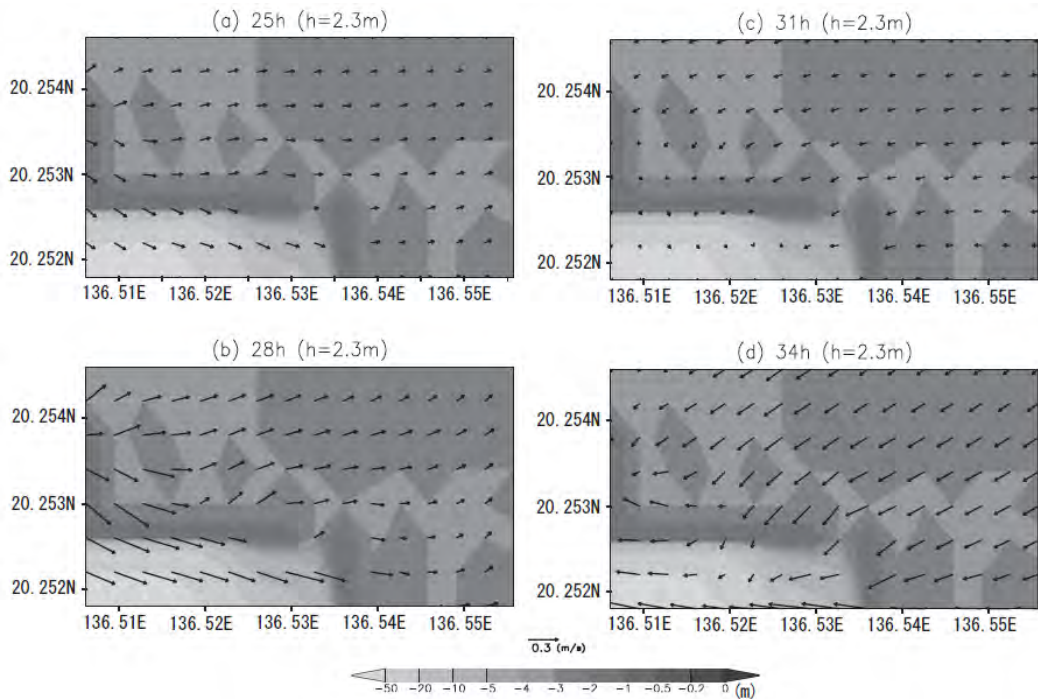


Figure 13: Sequence of a flow field around the channel.

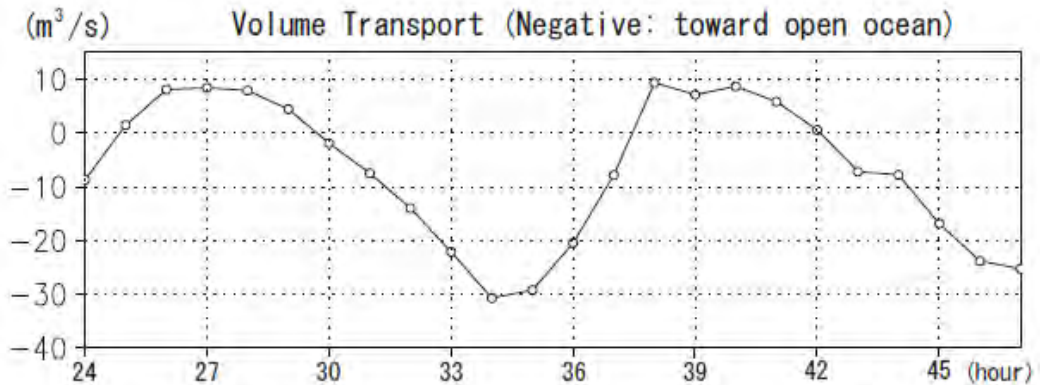


Figure 14: A time series of volume transport in the channel.

Figure 12 shows the velocity field in arrows at 35-hour (at ebb tide) at 2.3 m depth in the model with the bottom topography in shade. Water in the moat converges in the southwestern channel and is carried away out of the channel by the ebb tide. Figure 13 is the sequence of a flow field focused on the channel area. It is clearly seen that water spills out of the channel with the ebb tide and enters the moat with the flood tide, which indicates that the flow is dependant on the tide.

Figure 14 shows a time series of volume transport in the channel. The positive and negative signs show the transport directions, toward the reef and open ocean, respectively. Maximum in the ebb tide is higher than in the flood tide. The net volume transport in a day is approximately $161 \text{ m}^3/\text{day}$, which suggests that sand and gravel in the reef could be swept out of the channel.

6. Summary and Discussion

The characteristics of physical fields around a table reef as represented by Okinotorishima Island are investigated by use of the observed data and regionally idealised numerical models.

Observed data show that the sum of the 16 tidal constituents accounts for about 90 % of total variance in the record. Temperature difference between day and night at the point of observation is small compared with the previous study (Kumagaya et al., 2004). In the case of Shiraho reef, the reef area is hydrologically separated from open ocean around low tide and water cannot be exchanged between them. This is one of the reasons for high temperature during the daytime at Shiraho reef. At Okinotorishima Island, on the other hand, the small difference of temperature between day and night indicates that the reef area is continuously connected with the open ocean.

In order to estimate the relation between the thermal characteristics and susceptibility of coral to high temperature at Okinotorishima Island its spatial distribution in particular, we need long-term observation data for some points with the special characteristics of topography (e.g. channels and reef crests, etc).

Model results show that, by use of a model with an idealistic topography similar to a table reef and the nesting method, the experiment

with the horizontal resolution of 300 m is successful and the result from the model shows fine structures of the flow and temperature field around the island, which is not resolved by the coarse resolution model. The experiment with the JCOPE2 Reanalysis Data also succeeded in 900 m horizontal resolution model. However, the model with higher resolution cannot run, because of inappropriate setting of the boundary conditions. In order to compute finer horizontal resolution models, further observation for the initial and boundary conditions are needed.

An additional experiment using more realistic topography reproduced by a chart, observation data and the reanalysis data was performed. The results show that water is carried away out of the southwestern channel by the ebb tide and flows into the reef area with the flood tide. Taking the observation data into consideration, this indicates that the variation of flow field mainly depends on tidal variation. In the Shiraho reef, the dynamic balance between the radiation stress and wave setup around the reef crest plays a key role in the flow field in the reef area. In contrast to the flow field in the Shiraho reef, outflow from the reef similar to Okinotorishima Island is qualitatively explained by the tidal effects. In a reef with a topography in which the reef area could not be completely separated from the open ocean, such as Okinotorishima Island, radiation stress possibly has less effect on the characteristics of the flow field.

However, in order to estimate the ecological environment around Okinotorishima Island, this model must be improved. At the least, the following items are required to improve the model;

- 1) Checking the quality of the observed data,
- 2) Verifying the validity of the setting of the model domain,
- 3) Comparing observed data with model results in more detail,
- 4) Verifying boundary conditions from the model results to real conditions,
- 5) Examining dependence on the turbulence kinetic energy, eddy viscosities etc.,
- 6) Examining the validity of the steady state and temporal variations of numerical solutions, and
- 7) Verifying reproducibility from the numerical experiments.

More accurate results from more sophisticated models will be able to provide information for conservation and maintenance of natural resources at Okinotorishima Island. Furthermore, such models could be applicable to environmental conservation of other islands, particularly, to small island countries formed by reef islands. This study suggests a procedure of numerical simulation for outlying islands that tend to be highly vulnerable to sea level rise due to climate change and environment load due to human activities such as artificial land alteration, population increase, and pollution and garbage problems.

Acknowledgement

Observed data in Okinotorishima Island are supplied by JAMSTEC. The data from JCOPE2 reanalysis are supplied by the JCOPE group.

The author is deeply indebted to Associate Prof. Yukio Masumoto, Dr. Yasumasa Miyazawa, Dr. Hitoshi Tamura, and other members of the JCOPE group for all their fruitful advice.

References

- Ambe, D., K. Komatsu, M. Shimizu, and A. Okuno (2009): High precision mean sea-surface velocity field estimated by combining satellite altimeter and drifter data, submitted to Geophys. Res. Lett.
- Blumberg, A. F., and G. L. Mellor (1987): A description of a three-dimensional coastal ocean circulation model. Three-Dimensional Ocean Models, Ed., N. Heaps, Amer. Geophys. Union, 208 pp.
- Bryant, D., L. Burke, J. McManus and M. Spalding (1998): Reefs at Risk, Washington D. C.: World Resources Institute.
- Haney, R. L. (1991): On the Pressure gradient force over steep topography in sigma coordinate ocean models. J. Phys. Oceanogr., 21, 610-614.
- Kagimoto, T., Y. Miyazawa, X. Guo and H. Kawaji (2008): High resolution Kuroshio forecast system ? Description and its applications -, in High Resolution Numerical Modeling of the Atmosphere and Ocean, W. Ohfuchi and K. Hamilton (eds), Springer, New York, 209 ? 234.
- Kayanne, H., S. Harii, H. Yamano, M. Tamura, Y. Ide and F. Akimoto (1999): Changes in living coral coverage before and after the 1998 bleaching event on coral reef flats of Ishigaki Island, Ryukyu Islands, Galaxea, 1, 73-82 (Japanese).
- Kayanne, H., S. Harii, Y. Ide and F. Akimoto (2002): Recovery of coral population after the 1998 bleaching on Shiraho Reef, in the southern Ryukyus, NW Pacific, Mar Ecol Prog Ser., 239, 93-103.
- Mellor, G. L., and T. Yamada (1982): Development of a turbulence closure model for geophysical fluid problems. Rev. Geophys. Space Phys., 20 No.4, 851-875.
- Miyazawa, Y. and S. Minato (2000): Development of a two-way nesting code for the Princeton Ocean Model, JAMSTECR, 40, 11-22.
- Miyazawa, Y., T. Kagimoto, X. Guo and H. Sakuma (2008a): The Kuroshio large meander formation in 2004 analyzed by an eddy-resolving ocean forecast system, J. Geophys. Res., 113, C10015, doi:10.1029/2007JC004226.
- Miyazawa, Y., K. Komatsu and T. Setou (2008b): Nowcast skill of the JCOPE2 ocean forecast system in the Kuroshio ? Oyashio mixed water region (in Japanese with English abstract and figure captions), J. Marine Meteorol. Society (Umi to Sora)
- Oey, L. (2005): A wetting and drying scheme for POM, Ocean Modelling, 9, 135-150.
- Oey, L. (2006): An OGCM with movable land-sea boundaries, Ocean Modelling, 13, 176-195
- Oey, L., T. Ezer, C. Hu and F. E. Muller-Karger (2007): Baroclinic tidal flows and inundation processes in Cook Inlet, Alaska: numerical modeling and satellite observations, 57, 205-221
- Smagorinsky, J. (1963): General circulation experiments with the primitive equations, I, The basic experiment. Mon. Weather Rev., 91, 99-164.
- Spall, M. A. and W. R., Holland (1991): A nested primitive equation model for ocean application, J. Phys. Oceanogr., 21, 205-220.
- 熊谷航、田村仁、灘岡和夫、波利井佐紀、鈴木庸老、茅根創 (2004) : 石垣白保海域における水温環境特性と造礁サンゴ群集の分布、海岸工学論文集、51、1066-1070.
- 鈴木庸老、灘岡和夫、宮澤泰正、波利井佐紀、安田仁奈 (2004) : JCOPE および沿岸域モデルを用いたサンゴ・オニヒトデ幼生広域輸送特性の把握、海岸工学論文集、51、1146-1150.
- 田村仁、灘岡和夫、熊谷航 (2004) : 裾礁タイプサンゴ礁域における海水流動・温熱特性に関する数値シミュレーション、海岸工学論文集、51、1061-1065.
- 田村仁、灘岡和夫、Enrico Paringit (2004) : 石垣島東岸裾礁域の流動特性に関する現地観測と数値解析、土木学会論文集、768/II-68、147-166.

- 田村仁、灘岡和夫、鈴木庸彦、宮澤泰正、三井順
(2005) : 沖縄・石西礁湖自然再生計画立案の
ための熱・物質輸送数値シミュレーション、
海岸工学論文集、52、1161-1165.
- 灘岡和夫、波利井佐紀 (2004) : サンゴ幼生の広域
分散と海水流動物理過程、海洋と生物、152、
vol. 26 no.3、232-241.
- 三井順、灘岡和夫、鈴木庸彦、熊谷航、石神健二、
波利井佐紀、Enrico Paringit、田村仁、安田仁
奈、飯塚広泰、木村匡、上野光弘 (2004) : 沖
縄・石西礁湖における海水流動および濁質・
熱・サンゴ幼生輸送特性解明のための総合的
観測と解析、海岸工学論文集、51、1055-1059.

Joint Development of Mineral Resources on the Continental Shelf

Akari Nakajima*

Abstract

In accordance to the post-WWII advancement of maritime resource development technology and the extension of jurisdiction over waters, international disputes concerning maritime resources and maritime boundaries have increased. Some of these disputes, as the “Cod War” between Iceland the UK in the 1970s, may come to the point of armed conflict. Under these circumstances, states have attempted various methodologies of conflict resolution from bilateral negotiations to third party adjudication. The joint development of the continental shelf is one among these methods. Various states have employed this new option with neighboring states in order to settle disputes in the past. Also in recent eras, states have applied disputes regarding overlapping area of the extended continental shelf. This article aims to document state practices of joint development of mineral resources of the continental shelf and comprehend the status of joint development.

Key words: Joint Development (bilateral), Continental Shelf, Law of the Sea, Maritime Delimitation

* Ocean Policy Research Foundation